

# Advanced Hybrid Propellant for a Moon Orbiter Thruster

*L. L. Rossettini<sup>\*</sup>, F. Magistrelli<sup>\*</sup>, M. Mantegazza<sup>\*</sup>, L. Marini<sup>\*</sup>, L. DeCillia<sup>\*</sup>, A. Conti<sup>\*</sup>, P. Simontacchi<sup>\*</sup>, C. Renna<sup>\*</sup>, P. Mittino<sup>\*</sup>, G. Rapicano<sup>\*\*</sup>, G. Festa<sup>\*\*</sup>, L.T. De Luca<sup>\*</sup>, L. Galfetti<sup>\*</sup>, A. Russo Sorge<sup>\*\*</sup>, C. Carmicino<sup>\*\*</sup>*

*<sup>\*</sup> SPLab, Dipartimento di Energetica, Politecnico di Milano, I- 20156 Milan, Italy*

*<sup>\*\*</sup> DIAS, Dipartimento di Ingegneria Aerospaziale, Università degli Studi di Napoli "Federico II",  
I- 80125 Naples, Italy*

## Abstract

The Moon is the main objective for the next decade space missions. Exploitation, scientific research, robotic and manned exploration are planned by the most important space agencies. Just two transportation systems are currently used: liquid propellant and electric thrusters. The former has the advantage to be reliable and it has been tested in a wide range of missions, but it is heavy and complex, while the latter is usually lighter but it requires very long transfer time.

This study proposes a hybrid propellant thruster as the best compromise for lunar missions in which an orbiter should leave the transfer orbit and inject in a lunar orbit. The safety of the system, the simplicity of the architecture, the weight comparable with the electric thruster propulsion make the hybrid motor the best and the more convenient solution to reach the Moon.

*Keywords:* Aluminum Hydride, Metal Hydrides, Hybrid Propulsion, Moon Orbiter, Space Applications

## Introduction

The scenario described in this document represents a Moon Orbiter mission in which a 150 Kg spacecraft is launched as an auxiliary payload into a highly elliptical low inclination Geostationary Transfer Orbit (GTO) using the Ariane Support for Auxiliary Payloads (ASAP) by Ariane 5 or Soyuz from Kourou. A hybrid thruster is used to accomplish the lunar transfer and the lunar orbit insertion (200x200 Km) with a total  $\Delta V$  of 1080 m/s. Once in the Moon orbit several scientific objectives could be achieved. Total mission time once on the Moon: six months.

Hybrid propulsion is the best compromise between solid and liquid systems, joining advantages of both configurations: higher specific impulse compared to solid propellant, thrust control and re-ignition possibility, simpler architecture than liquid systems. Moreover, keeping separate fuel and oxidizer it greatly improves the safety of the entire system: chamber pressure can reach only the feeding pressure and no explosion can occur, possible defects and cracks of the solid grain have no consequences, solid fuel regression rate depends on the oxidizer mass flux and a higher value of the fuel mass flow rate involves only a different mixing ratio but not an uncontrolled pressure increase. There are also some disadvantages, such as low burning rate values and sensitivity (critical especially for large scale engines) and poor combustion efficiency.

The hybrid thruster designed in this study works with solid fuel and liquid oxidizer. The fuel is constituted by a polymer, Hydroxyl-terminated Polybutadiene, enriched with metal hydrides. The oxidizer is nitrous oxide (N<sub>2</sub>O), chosen mainly for its safety and low cost, although good performance are previously demonstrated [1][2][3]. The engine reaches a specific impulse of 300s and more, with 400N of thrust. The three main  $\Delta V$ s are split in several burning phases to avoid thermal issues, so the thruster has a reusable ignition system on-board.

Filament winding technology, widely used in Vega launcher for example, is proposed for both the case and the oxidizer tanks, and the total weight of the system is 75 Kg.

This hybrid thruster is believed to be a better solution than both the liquid bipropellant and electric engine systems for this mission. The performance are comparable to the no cryogenic liquid thruster while the hybrid system is lighter, safer and presents simpler architecture; the weight is comparable with the electric system, without Van Allen belts radiation problems and it requires much less power, so decreasing costs.

## Engine description

The spacecraft primary propulsion system consists of the hybrid propellant engine working with HTPB-based solid fuel enriched with metal hydrides and N<sub>2</sub>O oxidizer. This propulsion solution gives the optimum performance to

reach the final orbit in the least time, together with a low cost – high simplicity propulsion system. By adding energetic metal particles to solid fuel, energy release is augmented, density and specific impulse are increased, nozzle erosion is decreased, combustion instabilities may improve. Literature survey showed that this innovative formulation was never tested before in a fully functional hybrid rocket engine. In particular HTPB was chosen because it is widely used as fuel in hybrid rocket engines. Aluminum hydrides is fuels of relatively low density ( $1.477 \text{ gcm}^{-3}$ ) and large molecular mass ( $30.01 \text{ g mol}^{-1}$ ). Density is quite less than aluminium ( $2.70 \text{ gcm}^{-3}$ ) but they offer high density for hydrogen storage, about 10% hydrogen by mass, hence providing a higher density of hydrogen ( $0.148 \text{ gcm}^{-3}$ ) than liquid hydrogen ( $0.071 \text{ gcm}^{-3}$ ) [6]. Bulk  $\text{AlH}_3$  tends to dehydrogenate at room temperature after few hours, but the alpha phase of alane ( $\alpha\text{-AlH}_3$ ) has been observed to be stable while rapid dehydrogenation occurs at temperatures in between  $180\text{-}190^\circ\text{C}$  [7]. Thermochemical calculations show that replacing Al by the corresponding  $\text{AlH}_3$  results in both a lower flame temperature and a lower average molecular mass of the combustion products in solid propellants [4].  $\text{AlH}_3$  based propulsion application was indicated as a substantial gain for hybrid and solid rocket motors, especially for the upper stages of space launchers [9]. However, comparative analyses of transient combustion for metal hydrides based solid propellant were not found in literature. Overall, an increased (mass) specific impulse of about 20 s is found by comparing the two optimized formulations (AP/HTPB/Al vs. AP/HTPB/ $\text{AlH}_3$ ) [8]. The very limited volume and mass permitted by ASAP allocation pose constraints on tanks and case design. Moreover, thermal loads during the cruise phase to the moon force to use more than one tank for the oxidizer, connected to each other, to assure constant pressure between higher and lower temperature vessels. Oxidizer flux is controlled using pressure, flow and temperature transducers. A small axial injector atomize the  $\text{N}_2\text{O}$  into the pre-chamber. Ignitor system provide enough energy to start solid fuel decomposition. A simple, two layer, conical nozzle is proposed. In this work a selection between low cost solutions and high performance solutions are presented in every step of the engine design.

## Theoretical model

In the hybrid combustion chamber, an atomized or vaporized liquid flows down the port and reacts near the surface of the solid fuel. The controlling factors in combustion are the rate of heat transfer to the solid surface and the heat of decomposition of the solid phase fuel. The mass flux, which is regulated by the rate of flow of the liquid phase, determines the heat generated in the combustion zone and, hence, the heat transfer and thrust magnitude [1].

The combustion phenomenon is similar to that of a turbulent diffusion flame, for which the flame zone is established within the boundary layer. Process can conveniently be represented by an idealized model which treats the flame zone as a point of discontinuity in temperature gradient and composition. In the real case of finite combustion kinetics, the flame zone is thickened with continuous gradients in both temperature and composition. Oxidizer enters the flame zone from the port free stream core by diffusion, while the fuel enters the boundary layer as a result of vaporization at the wall surface. The combustion zone is established at that point where an approximate stoichiometric mixture has been achieved. This model shows that the combustion zone occurs within the turbulent boundary layer at a distance from the solid wall, which is less than the thickness of the momentum boundary layer. The axial velocity at the flame is also less than that at the outer edge of the boundary layer. This model was used to develop the mathematics of combustion [1] and derive the simplified regression rate law:

$$r = a_0 G_0^n$$

where  $n$  (depending on fluid dynamics) and  $a_0$  should be experimentally determined.

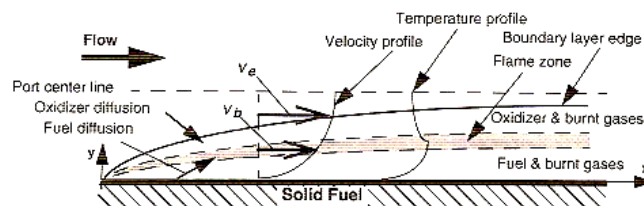


Figure 1: hybrid combustion diffusion flame structure

## Performance

Thermochemical computation was performed using CEA (produced by NASA [10][11]), ISP2001 (produced by Dr. Dunn [12]) and CPROPEP (based on code of Gordon and McBride [10]) softwares. Results were compared and used to map the engine performance at different formulations composition. In particular, chamber pressure of 1.5, 2 and 3 MPa was considered and nozzle expansion ratio of 50, 75 and 90. All the components content in the mixtures was varied from 0% up to 100% to completely describe formulation behaviour in terms of (mass) specific impulse and adiabatic flame temperature. An example is given in Figure 2 for AlH3 based formulation.

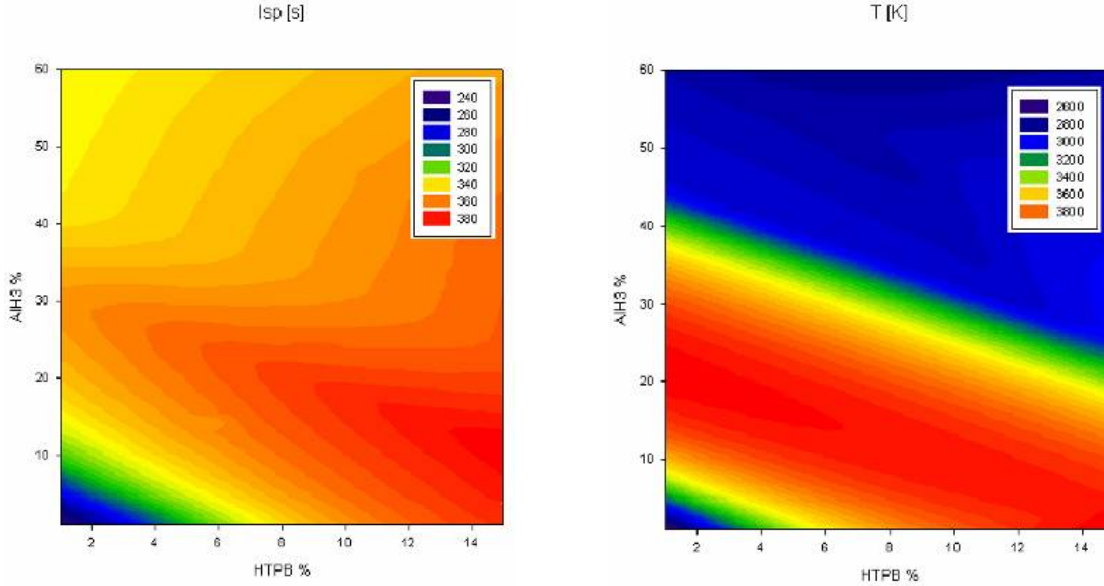


Figure 2: Example of performance calculation for HTPB-AlH3-N2O hybrid engine. Specific impulse map on the left and adiabatic flame temperature on the right

An optimization algorithm was generated to find the best range of components for the fuel and oxidizer / fuel best ratio. Only configurations which give a Isp greater than 300s were considered. The first of the main constraints considered in the optimization process was to keep the temperature as low as possible, to avoid thermal issues in the engine. Minimum allowable O/F was chosen to reduce the amount of oxidizer to store in the tanks: less and smaller tanks help to save mass of the entire system. For example, lowering O/F from 3.5 to 2, although the total propellant mass do not change, one tank less could be used and the mass saved could go up to 5 kg. Metal hydrides content was kept as low as possible to avoid potential fuel mechanical issues and to keep the fuel cost low. Moreover, gradient of Isp and T were minimized: fuel manufacturing errors do not affect performance too much.

Table 1: Performance of hybrid propellant based on different energetic additives after formulation optimization

	95% Isp, s	T, K	HTPB(R45)	Metal/Hyd.	N <sub>2</sub> O
<b>Al</b>	295.70	3920.08	10.00	25.50	64.50
<b>AlH3</b>	315.44	2953.99	10.28	25.15	64.57
<b>MgH2</b>	279.79	2421.68	19.80	15.80	64.40

Considering the total  $\Delta V$  required to accomplish the mission, Tsiolkovsky law [13] gives about 47kg of propellant required, 15.7kg of fuel and 31.4kg of oxidizer (2% margin included). However, in this calculation, 300s specific impulse was considered to take into account experimental uncontrolled variables which could lead to a performance decrease. Fuel grain constraints were mainly the maximum dimensions allowed for the entire engine, which should be placed in the Ariane ASAP adapter (0.8x0.7x0.7m). Single port grain length is 0.41 m with a port diameter of 0.14 m and external diameter of 0.25 m (O/F = 2) [14]-[25][28][30].

## Case and nozzle design

Usually three classes of materials are used: high-strength metals, wound-filament reinforced plastics and a combination of the formers. The strength-to-density ratio is better for composite materials which means that they have less inert weight, but on the other hand metals are cheaper. Although Aluminium 2219 is a metal with good mechanical properties, and also a low-density, in this work carbon-epoxy filament winding solution is presented. A winding operation is the basic fabrication technique for forming load-bearing structural elements made of polymer matrix-based fibrous composites, which have the shapes of bodies of revolution. By winding continuous strands of carbon fiber, fiberglass or other material in very precise patterns, structures can be built with properties stronger than some metals at much lighter weights.

Combustion chamber size is decided by the fuel grain dimensions. Pre-camera and post-camera are added. The pre-camera helps the oxidizer, injected into the motor, to vaporize providing a uniform entrance condition to the grain port. Oxidizer is largely gasified and heated before flowing down the port. For typical arrangements the length-to-diameter ratio is about 2.5 and 5. The post-camera allows to complete the combustion process. In fact, even with an optimum port length, it's usually the case that not all of the vaporised solid and liquid have been able to mix and burn before exiting the end of the port; the centre of the port tends to be fuel-lean whilst the flow at the wall fuel rich. Simply adding an empty space downstream of the port just before the nozzle is all that is required to recoup nearly all of this loss. As the flow exits the port, it goes over the edge where the grain ends causing a trapped toroidal vortex to occur, which mixes most of the flow before it encounters the nozzle. This post-combustion chamber is typically less than one chamber diameter in length: the extra chamber mass required is more than balanced by the increase in overall performance.

The motor case acts as a pressure vessel to contain the high pressure combustion processes occurring within the bore of the motor. It must be able to withstand the maximum chamber pressure under any possible operating condition. The pressure considered is 20 bar, but the calculation must account for normal variations about this value; in fact a safety factor must be introduced. Simple membrane theory is used to predict the state of stress in the case. For a cylinder, the longitudinal stress is one half of the tangential one. The maximum strain allowed by the material is the yield stress. Mariotte theory allowed to compute the correct case thickness.

The supersonic nozzle is the component in which the expansion of the hot gases occurs. It has to withstand a severe environment due to the great heat transfer and to the erosion phenomenon. In fact the nozzle converts high thermal energy of chamber gases to kinetic energy producing the highest velocities, heat transfers and pressure gradients. Advances in material technology allow substantial weight reduction. The structural part is made of primarily metals or some fiberglass. Metals have good structural and mechanical behaviour, sufficient resistance to the high stress environment. Erosion affects primarily the throat and the inlet section immediately upstream to it. Typically, in these regions, ablative materials with very low erosion rate, such as carbon-phenolic or carbon-carbon, are used. They are made of carbon fiber with a phenolic or carbon matrix to improve lifetime and erosion resistance. Relatively strong and lightweight, these materials can withstand temperatures up to 3400 K without losing their integrity.

A list of materials both for the supporting structure and for the insulator layer were carefully analyzed. Steel D64AC for the structural layer with carbon-phenolic insulator was selected as cheap solution, while fibreglass layered by carbon-carbon was chosen for its very convenient weight, although manufacturing and materials costs increase.

Quasi-one-dimensional nozzle flow theory was used to simplify the real aerothermochemical behaviour. However the assumptions stated are adequate to obtain useful solutions to the propulsion analysis [27]. Assuming that:

1. the flow is "frozen" (the products don't change in chemical composition while traversing the nozzle);
2. all the species of the working fluid are gaseous (solid or liquid phases have negligible mass);
3. products of combustion constitute a perfect gas;
4. the flow is adiabatic (heat transfers don't dissipate energy from the flow across the chamber walls);
5. the propellant flow is steady (transient effects are of short duration and can be neglected);
6. all the exhaust gases are axially directed;
7. the flow is one dimensional (properties are uniform across any normal section);
8. there is no friction and boundary layer effects are neglected;
9. there are no shock wave or any other discontinuity in the flow.

It is possible to design the nozzle, adapted to a pressure very close to vacuum: 1kPa. In order to limit the maximum length of the entire nozzle, due to allocation in the ASAP adapter, a converging angle of 60 degrees was chosen, while 15 degrees for diverging conical part as compromise in between nozzle performance and length. Mariotte theory was used to calculate the nozzle thickness in order to withstand the maximum stress tolerated by the material. A safety factor equal to 1.2 was used. Final design is described in (Table 3) with a 3D view.

Table 2: hybrid engine case dimension in the low cost (Aluminum) and low mass (filament winding) configurations

MATERIAL	Al 2219	Carbon/Epoxy
Case diameter, mm	266	266
Case thickness, mm	2.19	1.44
Camera length, mm	413.7	413.7
Post-camera length, mm	62.5	62.5
Pre-camera length, mm	62.5	62.5
<b>TOTAL LENGTH, mm</b>	<b>538.7</b>	<b>538.7</b>
Camera mass, kg	1.995	0.799
Post-camera mass, kg	0.320	0.121
Pre-camera mass, kg	0.320	0.121
<b>TOTAL MASS, kg</b>	<b>2.763</b>	<b>1.041</b>

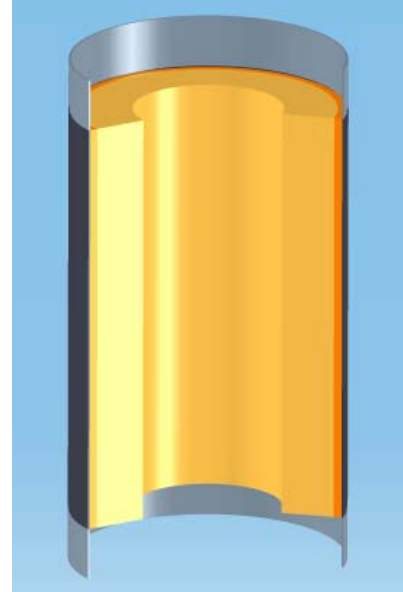
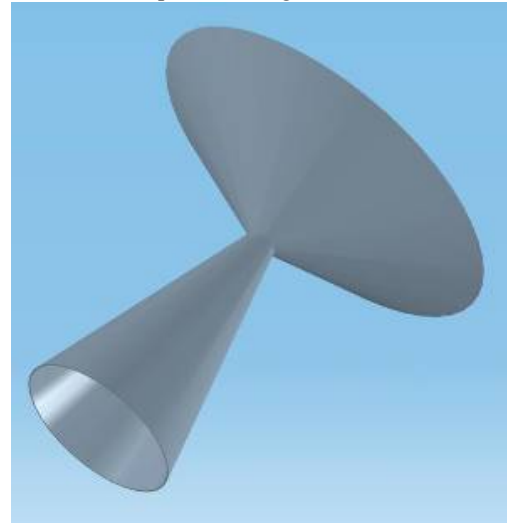


Table 3: Final nozzle design for metal but cheap solution and composite and light solution

	Steel D6AC	Fiberglass
Convergent length, mm	73.50	73.50
Divergent length, mm	129.6	129.6
Thickness, mm	0.377	0.520
<b>TOTAL LENGTH, mm</b>	<b>203.1</b>	<b>203.1</b>
Convergent diameter, mm	266.00	266.00
Divergent diameter, mm	80.90	80.90
Throat diameter, mm	11.40	11.40
Convergent mass, kg	0.094	0.033
Divergent mass, kg	0.055	0.019
<b>TOTAL MASS, kg</b>	<b>0.15</b>	<b>0.053</b>



### Oxidizer feeding system

The selected to work with the fuel described before is N<sub>2</sub>O which has a self-pressurizing capability depending on the temperature [35]. This particular feature permits to save weight eliminating pressurizing systems and diaphragms in the tanks. Moreover, N<sub>2</sub>O is a very innocuous gas, very easy and safe to handle and compatible with several different materials, from aluminum to composites. Oxidizer is stored in 4 identical aluminum tanks, positioned parallel to the engine on the four corners. Although composite tanks would have lead to a significant decrease in mass, space certification process required to fly the engine in Ariane5 rockets needs at least two years and several tanks to test. Not only this could shift the mission launch date but also increase significantly the overall costs. Of the shelf tanks were individuated with a capacity of 14.25 liters each. The surplus volume available is used to control the increase of pressure due to temperature when one or two tanks are exposed to the sun during the cruise phase. In fact, all the tanks are connected to each other to assure a constant and equal pressure in all the oxidizer feeding system (Figure 3).

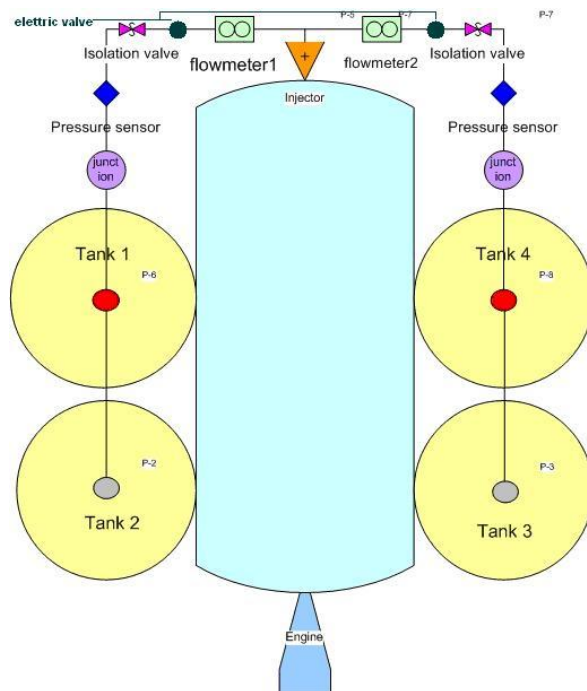


Figure 3: Oxidizer feeding system scheme

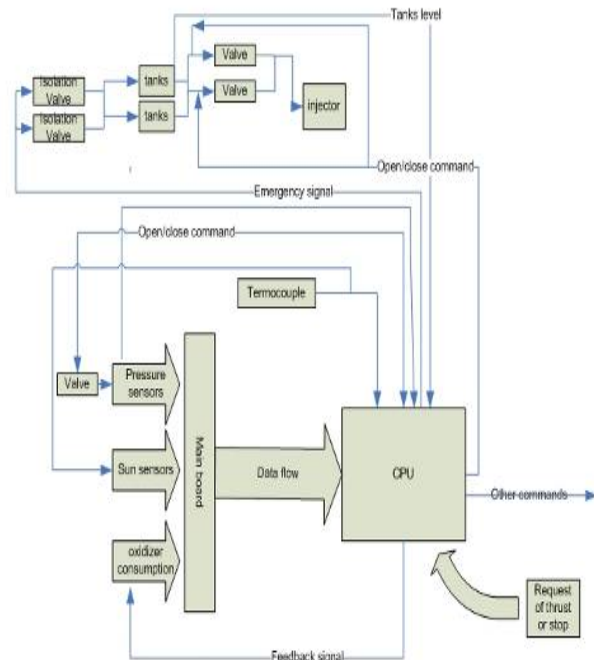


Figure 4: loop control of oxidizer flux into the engine

Redundancy assures system will work even in case of one of the two flux regulator failure and interconnection of the tanks permits N<sub>2</sub>O to flow even if some of the ¼" aluminum pipes does not work properly. Safety is guarantee by two isolation valves and all the system is monitored by flow, temperature and pressure sensors which are used by the flow control system to pilot the N<sub>2</sub>O flux in the combustion chamber (Figure 4) [26][45]. Moreover, temperature sensors are used also by central satellite OBDH to control heaters on the tanks which have the task to keep the temperature as constant as possible during engine firing: flow of oxidizer causes a significant drop of pressure which could lead to performance losses. On the top part of the pre-chamber a flange hosts the oxidizer injector. The injector plate is designed to provide the desired flow rates into the thrust chamber transforming the liquid oxidizer into gas (atomization). Injector holes are positioned in a radial showerhead pattern to distribute the flow evenly across the fuel port (Figure 5).

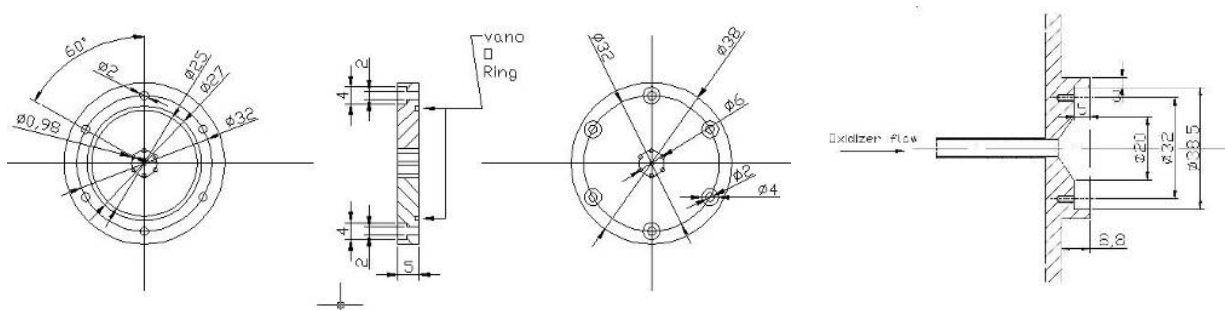


Figure 5: External, section, internal and lodging view of the injector plate

Although material chosen is steel AISI 316 the overall weight of the injector is about 50g due to its small dimensions.

## Multiple ignition system

An hybrid rocket motor is turned on by a source of heat that makes the gasify the solid fuel [44]. Then, introduction of the oxidizer let the flame spread in order to fully ignite the grain [38]. The ignition is typically obtained with the



injection of an hypergolic fuel in the combustion chamber. Small hybrid motors, however, are often electrically ignited by joule effect through a resistor, such as steel wool, located in the combustion port, or by use of a propane or hydrogen ignition system. A very interesting option use a catalyzer to decompose the oxidizer and to ignite the solid grain [41][37][36].

Two different ignition system were compared: catalytic and sparks generator.

Thermal decomposition of  $N_2O$  usually occurs at about 1270K while in the catalyzed system decomposition temperature could be decreased to about 470K. Using about 35W it is possible, in few seconds, start the engine using a 30-40%  $Ir_2O_3 / Al_2O_3$  catalyzer [40][42]. However some relevant data were found in literature, a working catalyzed ignition system applied to a hybrid engine was not found [48]. Moreover catalyzer materials could be very expensive and, in some cases, toxic [46].

A simpler solution is represented by a sparks generator constituted by another gas, propane  $C_3H_8$  [43], injected together with  $N_2O$  in the pre-chamber, and ignited using a spark (Figure 6).

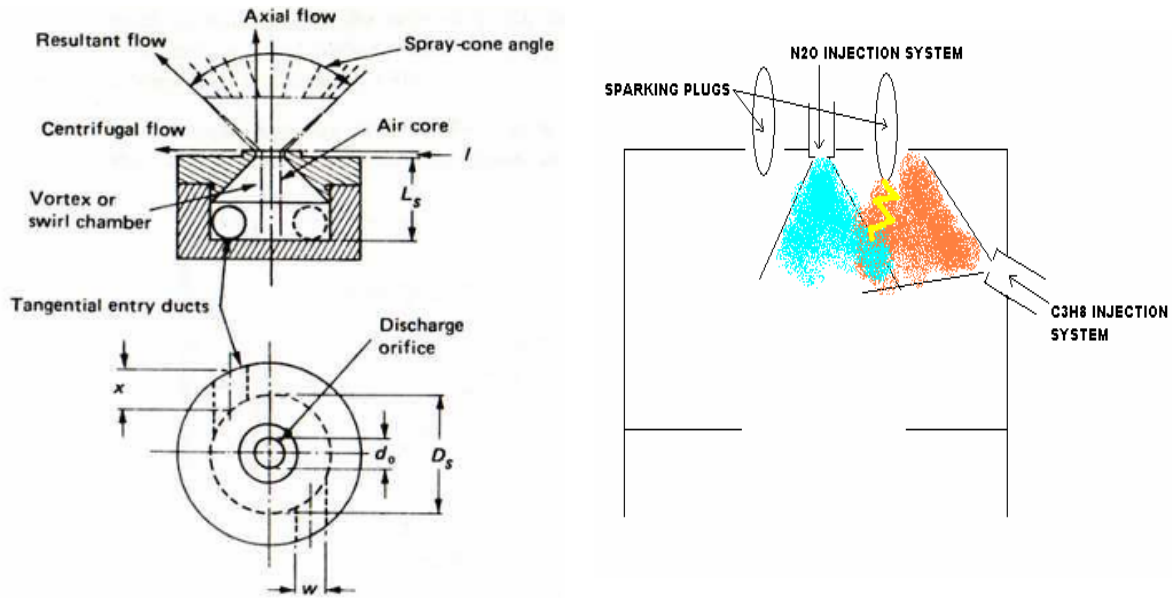
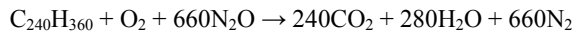
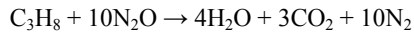


Figure 6: on the left:  $C_3H_8$  injector; on the right: ignition scheme

The simplest form of pressure-swirl atomizer (simplex atomizer) is used. Fuel is fed into the swirl chamber through tangential ports that give the fuel a high angular velocity, thereby creating an air-cored vortex. The outlet from the swirl chamber is the final orifice and the rotating liquid flows through this orifice under both axial and radial forces to emerge from the atomizer in the form of a hollow conical sheet. The stoichiometric reaction propane/nitrous-oxide produces enough heat to ignite the solid fuel grain [29]. Cpropep software calculation of the two reactions:



shows balanced reaction heat. Assuming a power density of  $30W/cm^2$  and a combustion area of about  $1420 cm^2$ , a power of 42.6kW is need to ignite the grain. According to the stoichiometric reaction 2.8g/s of propane and 27.3g/s of nitrous oxide are needed for no more than one second every firing. Considering the worst case of 15 ignitions, 42g of propane and 400g of nitrous oxide are needed.

### Thermal behaviour analysis

The scope of this analysis is to predict the temperature profile in the grain of fuel, with particular care to the wall temperature, during the burning rate, to avoid damages to combustion chamber [48][49][50]. Ablative material thickness is calculated to prevent wall case fusion during the three burning time, respectively of 280 s, 40 s, 80 s.

Calculations are performed assuming the grain temperature initially at 283 K, while when the combustion starts a uniform temperature of 3000 K on the combustion grain side. This very conservative situation permits to take into account ignition transitories, combustion profiles and some margin.

A finite difference method is used to predict temperature profile:

$$\frac{\partial^2 T}{\partial r^2} + \frac{1}{r} \cdot \frac{\partial T}{\partial r} = \frac{1}{\alpha} \cdot \frac{\partial T}{\partial t} \Rightarrow \begin{cases} \frac{T_{i+1}^n - 2 \cdot T_i^n + T_{i-1}^n}{\Delta r^2} + \frac{1}{r_i} \cdot \frac{T_{i+1}^n - T_{i-1}^n}{2 \Delta r} = \frac{1}{\alpha} \cdot \frac{T_i^{n+1} - T_i^n}{\Delta t} \\ r_i = (i-1) \Delta r \\ Fou = \frac{\alpha \cdot \Delta t}{\Delta r^2} \\ T_i^{n+1} = T_i^n + Fou \cdot (T_{i+1}^n - 2 \cdot T_i^n + T_{i-1}^n) + \frac{Fou}{2 \cdot (i-1)} \cdot (T_{i+1}^n - T_{i-1}^n) \end{cases}$$

First two ignitions do not constitute a problem for the case, and one millimeter of fuel grain could isolate the engine also during the third shot, avoiding also conductive heat coming from post-chamber. Pre-chamber has a low temperature and insulation is not required, while post-chamber, in which hot gases are mixed, requires an ablative material or insulating liner. Using 15mm of carbon phenolic liner [31][52] and supposing to have all the burnings in a continuous sequences for 300 s the external post-chamber material does not reach dangerous temperature (Figure 7). Insulation total weight is 1.5 kg.

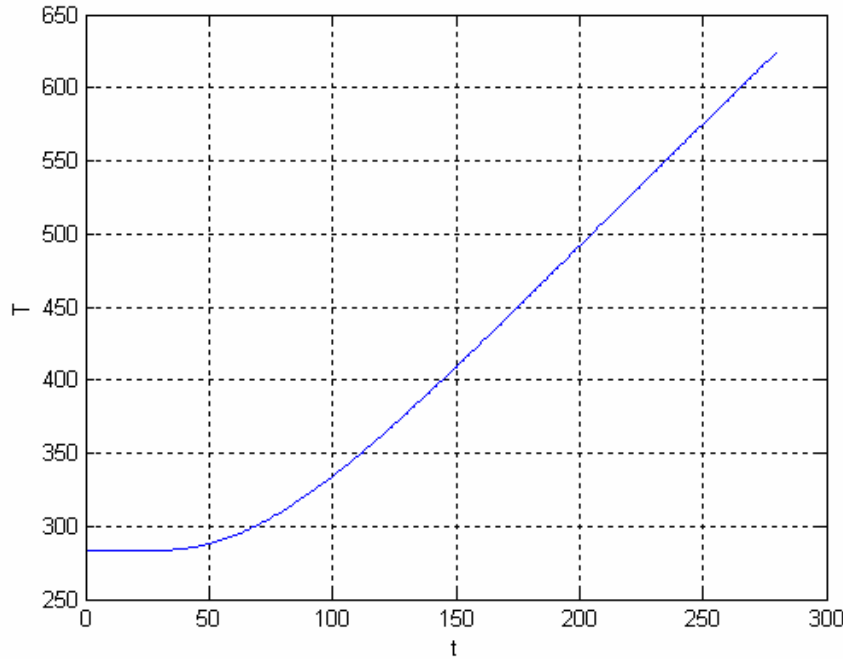


Figure 7: thermal profile on the external side of the liner after 300 sec

## Conclusions

A Hybrid engine as chemical propulsion option to bring a satellite from a GTO orbit to a final orbit around the moon is presented. Solid fuel – liquid oxidizer type engine was chosen. Metal hydrides additives in the solid fuel guarantees a specific impulse greater than 300 s and engine thrust of 400 N. Optimizations were done to find the best performance of propellant mixture in terms of performance, temperature and volume occupied by fuel and oxidizer to fully accomplish all the constraints coming from the other satellite subsystems. Grain shape was designed and engine dimensions and materials properly adapted: two materials sets were proposed, both of them satisfying launch



stress and pressure stress issues. One set is particularly suited to save money, the second to save mass. Nozzle and injector plate were designed to take into account chamber pressure and tank pressure. Oxidizers feeding system components were selected off the shelf to avoid space-certification. Particular care was put on redundancy issues. Heaters should be provided by satellite thermal subsystem to heat the tanks during firing. Multiple ignition systems were analyzed and, although a very promising catalytic system was reported, a simple spark-igniter was selected to avoid space certification time and costs.

Thermal combustion behavior was studied to take into account heat flux during combustion and accomplish constraints from both mission analysis requests in terms of minimum burning time and AOCS requests in terms of maximum burning time. Firing test during real mission should be performed to eventually correct thruster misalignment. Total mass of the chemical propulsion system is about 75 kg while the peak power used during combustion is less than 30 W.

Although very precise calculations were done in this work an experimental session is strongly suggested to study pressure profile during combustion, real specific impulse and overall engine performance.

## References

- [1] Sutton, G.P., Biblarz, O., Rocket propulsion elements, *Wiley Interscience*, Seventh edition, USA, 2001
- [2] Altman, D., Highlights in Hybrid Rocket Propulsion, *Proceeding 10-IWCP*, edited by L.T. DeLuca
- [3] Williams, G., Macklin, F. and Sarigul-Klijn, M., Almost there: responsive space, *2nd Responsive Space Conference*, April 19–22, Los Angeles, CA, 2004
- [4] DeLuca, L.T., Galfetti, L., Severini, F., Rossetini, L., Meda, L., Marra, G., D'Andrea, B., Weiser V., Calabro M., Vorozhtsov, A.B., Glazunov A.A. and Pavlovets G.J. Physical and ballistic characterization of AlH<sub>3</sub>-based space propellants. *Aerospace Science and Technology*, vol. 11, n°1, January 2007
- [5] Thome, V., Kempa, P.B. and Herrmann, H., Structure chemical and physical behavior of aluminum hydride. *Proceedings ICT 2003*, Paper P-104, 2003
- [6] Bazyn, T., Eyer, R., Krier, H. and Glumac, N., Dehydrogenation and burning of aluminum hydride at elevated pressures, *AIAA Paper* 2004-789, 2004
- [7] Chan, M.L. and Johnson, C.L., Evaluation of AlH<sub>3</sub> for propellant application, *Proceedings 8-IWCP*, edited by L.T. DeLuca, Grafiche GSS, Bergamo, Italy, Paper 33, 2003
- [8] Glumac, N., Krier, H., Bazyn, T. and Eyer R., The combustion characteristics of aluminum hydride under solid rocket motor conditions, *Proceedings 9-IWCP*, edited by L.T. DeLuca, L. Galfetti, and R.A. Pesce-Rodriguez, Grafiche GSS, Bergamo, Italy, Paper 46, 2004
- [9] Calabro, M., LOX/HTPB/AlH<sub>3</sub> hybrid propulsion for launch vehicles boosters, *AIAA Paper*, 2004-3823, 2004
- [10] Gordon, S. and McBride, B. J., Computer Program for Computation of Complex Chemical Equilibrium Compositions, Rocket Performance, Incident and Reflected Shocks, and Chapman-Jouguet Detonations, *NASA SP-273*, 1971
- [11] McBride, B. J., Zehe, M. J. and Gordon, S. , NASA Glenn Coefficients for Calculating Thermodynamic Properties of Individual Species, *NASA TP-2002-211556*, September 2002
- [12] Dunn, B.P., Rocket Engine Specific Impulse Program, [www.dunnspace.com](http://www.dunnspace.com), 2001
- [13] Tsiolkovsky, K.E., The Exploration of Cosmic Space by Means of Reaction Devices, 1903
- [14] Ziliac, G. and Karabeyoglu, A., Hybrid Rocket fuel regression rate data and modelling, *42nd AIAA/ASME/SAE/ASEE Joint Propulsion Conference & Exhibit*, AIAA 2006-4504, July 2006
- [15] Ziliac, G., Lohner, K., Dyer, J., Doran, E. and Dunn, Z., Fuel Regression Rate Characterization Using a Laboratory Scale Nitrous Oxide Hybrid Propulsion, *42nd AIAA/ASME/SAE/ASEE Joint Propulsion Conference and Exhibit*, Sacramento, California, July 9-12, 2006
- [16] George, P., Krishnan, S., Varkey, P.M., Ravindran, M. and Ramachandran, L., Fuel Regression Rate in HTPB / GOX Hybrid Rocket Motors, *AIAA/ASME/SAE/ASEE Joint Propulsion Conference and Exhibit*, 34th, Cleveland, OH, July 13-15, 1998
- [17] Serin, N. and Gogus, Y.A., Navier-Stoke investigation on reacting flow field of HTPB/O<sub>2</sub> hybrid motor and regression rate evaluation, *39th AIAA/ASME/SAE/ASEE Joint Propulsion Conference and Exhibit*, Huntsville, Alabama, July 20-23, 2003
- [18] Carmicino, C., and Russo Sorge, A., Influence of a Conical Axial Injector on Hybrid Rocket Performance, *Journal of Propulsion and Power*, Vol. 22, No. 5, 2006, pp. 984-995
- [19] Evans, B., Risha, G.A., Favorito, N., Boyer, E., Wehrman, R.B. and Libis, N., Instantaneous Regression Rate Determination of a Cylindrical X-Ray Transparent HR, *39th AIAA/ASME/SAE/ASEE Joint Propulsion Conference and Exhibit*, 20-23 July 2003, Huntsville, Alabama
- [20] De Zilwa, S., Ziliac, G., Karabeyoglu, A. and Reinath, M., Time-Resolved Fuel-Grain Regression Measurement in HR, *39th AIAA/ASME/SAE/ASEE Joint Propulsion Conference and Exhibit*, 20-23 July 2003, Huntsville, Alabama

- [21] Karabeyoglu, M. , Cantwell, B.J. and Ziliac, G., Development of scalable space-time averaged regression rate expression for HR, *41st AIAA/ASME/SAE/ASEE Joint Propulsion Conference and Exhibit*, Tucson, Arizona, July 10-13, 2005
- [22] Frederick, Jr. R.A. and Moser, M.D., Regression Rate Study of Mixed Hybrid Propellants, *41st AIAA/ASME/SAE/ASEE Joint Propulsion Conference and Exhibit*, Tucson, Arizona, July 10-13, 2005
- [23] Serin, N. and Gogus, Y.A., Fast computer code for hybrid motor design, EULEC, and results obtained for HTPB/O<sub>2</sub> combination, *AIAA-2003-4747*, 2003
- [24] Rajesh, A., Kuznetsov, A. and Natan, B., Design of a Lab-Scale Hydrogen Peroxide/HTPB HR, *39th AIAA/ASME/SAE/ASEE Joint Propulsion Conference and Exhibit*, 20-23 July 2003, Huntsville, Alabama
- [25] Chiaverini, M.J., Kuo, K., Peretz, A. and Harting, G.C., Regression-Rate and Heat-Transfer Correlations for HR combustion, *Journal of Propulsion and Power*, Vol. 17, No.1, Jan-Feb 2001, pp. 99-110
- [26] Casalino, L. and Pastrone, D., Oxidizer control and optimal design of hybrid rockets for small satellites, *Journal of Propulsion and Power*, vol.21 no.2, 2005
- [27] Sternin, L.E., Calculating the thrust characteristics of Nozzles, *Fluid Dynamics*, Volume 38, Number 1, January 2003
- [28] Carmicino, C., and Russo Sorge, A., Role of Injection in Hybrid Rockets Regression Rate Behavior, *Journal of Propulsion and Power*, Vol. 21, No. 4, 2005, pp. 606-612
- [29] Zakirov, V., Richardson, G. and Sweeting, M., Surrey Research Update on N<sub>2</sub>O Catalytic Decomposition, *AIAA/ASME/SAE/ASEE Joint Propulsion Conference and Exhibit*, 37th, Salt Lake City, UT, July 8-11, 2001
- [30] Martinez-Sanchez, M., Some Examples of Small Solid Propellant Rockets for In-space Propulsion, lecture 9
- [31] Mirmira, S.R., Jackson, M.C. and Fletcher L.S., Effective Thermal Conductivity of Graphite Fiber Composites, *Journal of Thermophysics and Heat Transfer*, vol.15 no.1, 2001
- [32] Lefebvre, A.H., Gas turbine combustion, *Hemisphere Publishing Corporation*, 1983
- [33] Kuo, K.K., Principles of combustion, Wiley, 1986
- [34] Glassmann, I., Combustion, Academic Press, 1977
- [35] Zakirov, V.A. and Li L., 1D Homogeneous liquefied gas self-pressurization model, *Proceeding of European Conference For Aerospace Sciences (Eucass)*, July 2005
- [36] Zakirov, V.A. and Ke Wan, N<sub>2</sub>O propulsion research at Tsinghua: 2006, *Proceedings of ESA Space Propulsion Conference*, September 2006
- [37] Zakirov, V.A. and Luming Li, N<sub>2</sub>O propulsion research at Tsinghua: 2003, *Proceedings of the 2nd International Conference on Green Propellants for Space Propulsion*, June 2004
- [38] Zakirov, V.A. and Ke Wan, Restartable hybrid rocket motor using nitrous oxide, *IAC-06-C4.2.02*
- [39] Zakirov, V.A. and Luming Li, Prospective N<sub>2</sub>O monopropellant for future small satellite dual-mode propulsion, *Proceedings of International Symposium on Space Propulsion*, August 2004
- [40] Pieterse, J.A.Z., Booneveld, S. and Van Den Brink R.W. Evaluation of Fe-Zeolite catalysts prepared by different methods for the decomposition of N<sub>2</sub>O, *Applied Catalysis B: Environmental*, Vol.51, No.4, 215-228, 2004
- [41] Tiliakos, N. and Tyll, J.S., Development and testing of a nitrous oxide/propane rocket engine, *AIAA 2001-3258*
- [42] Schneider, S.J. and Boyarko, G.A., Catalyzed combustion of bipropellants for micro-spacecraft propulsion, *AIAA 2003-4924*
- [43] Balasubramanyam, Moser and Sharp, Catalytic ignition of nitrous oxide with propane/propylene mixtures for rocket motors, *AIAA 2005-3919*
- [44] Kozakai, Tanabe and Kuwahara, Ignition characteristics of gas hybrid rocket, *AIAA 2006-4346*
- [45] Rajesh K.K., Thrust modulation in a nitrous oxide/hydroxyl polybutadiene hybrid rocket motor, *AIAA 2006-4503*
- [46] Kappenstein, Brahmi and Amariei, Catalytic decomposition of energetic compounds – influence of catalyst shape and ceramic substrate, *AIAA 2006-4546*
- [47] Barley and Palmer, Evaluating the miniaturisation of a monopropellant thruster, *AIAA 2006-4549*
- [48] Vernimont, E.J. and Heister, S.D., Combustion experiments in hydrogen peroxide / polyethylene Hybrid rocket with catalytic ignition, *AIAA 2000-5571*
- [49] Valentian, D. and Sippel, M., Green propellants options for launchers, manned capsules and Interplanetary missions , *Proceedings of the 2nd International Conference on Green Propellants for Space Propulsion*, 2004
- [50] Karam, R. D., Satellite thermal control for system engineers, *Progress in Astronautics and Aeronautics*, vol. 181
- [51] Guglielmini and Pisoni, Elementi di trasmissione del calore, *edited by cea ambrosiana*, 2000
- [52] Awam, I.S., Optimization of ablative composites thermal protection layer for high temperature aerospace applications, *International Bhurban Conference on Applied Sciences and Technology*, presentation



This page has been purposely left blank